Numerical Characterization of Rodent Exposure Imbalances in Large Reverberation Chambers

Numerical Characterization of Rodent Exposure Imbalances in Large Reverberation Chambers

A. Faraone[1], G. Bit-Babik[1], K. Sanderson[2], P. Russo[3], A. De Leo[3], V. Mariani Primiani[3], V. De Santis[*4]

[1]Motorola Solutions, Fort Lauderdale, United States
[2]University of Illinois, Urbana-Champaign, United States
[3]Università Politecnica delle Marche, Ancona, Italy
[4]University of L'Aquila, L'Aquila, Italy [*]valerio.desantis@univaq.it

***Abstract* — In the past two decades, reverberation chambers (RCs) have been increasingly utilized in large-scale rodent bioassays to study dose-response relationships for cancer and non-cancer biological endpoints. Computational radio-frequency (RF) dosimetry plays a critical role in the design of these studies, influencing key parameters such as RC size, number, cohort size, and exposure frequencies. Given the complexity of modeling animal-loaded RCs, simplified random plane-wave (PW) superposition techniques have often been used, though full-wave characterizations have also been explored. This study expands previous research by analyzing the effects of line-of-sight (LoS) elimination in the Università Politecnica delle Marche RC at 900 MHz, modeling 96 caged rodents. Using whole-body Specific Absorption Rate (wbSAR) as the key observable, the study highlights asymmetries in RC exposures, showing higher wbSAR values near the mode-stirrer. The study investigates field diffusers and cage repositioning strategies to mitigate these imbalances. Simulations conducted with Transmission-Line Matrix (TLM) and Finite Element Method (FEM) techniques reveal a weaker correlation between wbSAR and rodent mass than previously reported. These findings suggest that real-world RC configurations introduce exposure variations not necessarily captured by idealized Rayleigh field models, impacting the interpretation of rodent bioassay results.**

***Keywords* — imbalances, numerical dosimetry, reverberation chamber (RC), rodent bioassay, specific absorption rate (SAR).**

I. Introduction

Over the last two decades, reverberation chambers (RCs) have increasingly been employed in large-scale lifetime rodent bioassays [1]-[5]. Study protocols frequently require setting a number of exposure levels, including sham exposure for distinct animal cohorts, in order to appreciate any dose-response relationships relative to a large variety of cancer and non-cancer biological endpoints. Normally, a statistically significant dose-response relationship would be deemed to strengthen any findings.

Radio-frequency (RF) numerical dosimetry studies applied to large rodent cohorts inside RCs have consequently taken a prominent role in designing and interpreting the study outcomes. Particularly in the design phase of a study, in the absence of any physical RC model yet, computational RF dosimetry may assume a prominent role in directing some key design choices, like RC size and number, cohort size, RF exposure frequencies, etc., with enormous impact on the study cost, logistics, and – more importantly – the eventual statistical power and human applicability of any findings.

Due to the inherently large RC electrical domain, applying computational techniques to the analysis of animal-loaded RCs has proven quite challenging, pushing towards the adoption of simplified RC fields representations by means of random plane-wave (PW) superposition [6]-[10]. Nevertheless, there are also studies reporting full-wave characterization of rodent-loaded RCs, featuring the modelling of small-size [11]-[12] and more recently large-size [13] RCs including mode-stirrers and antennas. The practical implementation of this comprehensive characterization hinges on powerful computers.

In this study, we expand the preliminary investigations at 900 MHz presented in [13] by considering line-of-sight (LoS) from the animal cages, making it possible to "hide" the antenna behind the RC mode-stirrer (NLos), effectively eliminating LoS illumination. As in the preliminary investigation, the Università Politecnica delle Marche, Italy, RC (UNIVPM-RC) [14] was modeled in time-domain as well as in frequency-domain in conjunction with the 96 caged rodent models introduced in [10].

Adopting the whole-body Specific Absorption Rate (wbSAR) as the key observable, as in most prior RC dosimetry studies [1]-[13], we also documented the cage-wise ensemble-averaged wbSAR imbalances due to inherent asymmetries in a real RC, as compared with the ideal symmetries artificially enforced when idealized Rayleigh fields are impressed in the computational domain through random PW superposition [15], suggesting consistently higher exposures in cages that are closer to the RC mode-stirrer. To mitigate such imbalances, we studied the impact of "field diffusers" affixed to the RC walls, as well as the introduction of translational or rotational dynamic positioning of the cage assembly within the constraints of a realistic RC. Finally, the correlation between wbSAR and rodent mass has been documented in all studied cases, differing substantially from prior estimates based on PW superposition.

II. Models and Methods

The computational RF dosimetry study focused on a frequency of 900 MHz, consistent with our previous works [10], [13], which was the carrier frequency employed in the US National Toxicology Program (NTP) rats bioassays [3]-[4]. Utilizing the Simulia CST Studio Suite allowed for both time- and frequency-domain analyses. The Transmission-Line Matrix (TLM) method was employed for the time-domain analysis, while the Finite Element Method (FEM) was used for the frequency-domain analysis. Both methods support conformal

meshing and enable the relaxation of the mesh at greater distances from the high-permittivity rat models, which helps manage simulation times within a multivariate Monte Carlo (MC) framework. TLM is particularly effective for characterizing instantaneous wideband behaviors; however, for computational efficiency, the FEM analysis was conducted at a single frequency. The current FEM implementation in CST Studio provides mesh refinement based on the convergence criteria for wbSAR, while the TLM method depended on the convergence of the electric field at specified points within the rat models. This dual-method approach is intended to provide greater confidence in the applicability of the computational dosimetry results during the bioassay design.

A. RC Modeling

Figure 1(a) depicts the UNIVPM-RC chamber, a full-revolution mode-stirrer, a discone antenna, and 96 rat models housed in polycarbonate cages arranged in a 6×4×4 lattice along the *u*, *v*, *w* directions, respectively. The chamber measures about 3 m × 4 m × 2.5 m (*u*, *v*, *w* axes). The cage assembly volume is approximately 1.65 m × 1.58 m × 1.14 m in the static arrangement depicted, as well as in the translational dynamic arrangement illustrated in the following. However, in order to fit within the available RC area while ensuring the cages would keep at least a quarter-wavelength ($\lambda/4$) away from the RC walls, the cage assembly was also rearranged in a 4×4×6 lattice, occupying approximately a 1.09 m × 1.58 m × 1.76 m volume in the rotational dynamic arrangement depicted in Figure 1(b).

The same antennas described in [13], i.e., electrically-large (horn) and -small (U-shaped dipole and discone) antennas, as shown in Figure 2, were alternatively positioned LoS (horn) or between the mode-stirrer and the RC back wall, so as to avoid LoS illumination of the cages, for the latter. All antenna scattering parameters were normalized to 50 Ω in order to calculate the net RF power into the RC. Furthermore, we studied the potential impact of hemispherical "field diffusers", arranged in rectangular arrays of grounded metallic scatterers across three RC walls as shown in Figure 1(a). The diffusers used in this study all have same radii equal to $\lambda/2\pi$ at 900 MHz and are spaced one wavelength apart. The RC walls, floor and ceiling, the mode-stirrer, diffusers, and the metallic antenna parts were modelled as annealed copper ($\sigma = 5.8 \times 10^7$ S/m), while dielectrics were modelled as lossless.

B. Rat Modeling

This study utilized four homogeneous, untailed rodent models, characterized by properties derived from [7]: a mass density of $\rho = 1000$ kg/m^3, conductivity of $\sigma = 0.95$ S/m, and relative permittivity of $\varepsilon_r = 40$. Previous research [10] has demonstrated that these models effectively replicate the wbSAR of the corresponding anatomical models. The cages were constructed from 3 mm thick lossless polycarbonate ($\varepsilon_r = 2.9$), maintaining the external dimensions specified in [10] (23.5 cm × 26 cm × 21 cm in the *u*, *v*, and *w* axes), as well as the same horizontal (5 cm in the *u* and 18 cm in the *v* directions) and vertical (10 cm in the *w* direction) spacings.

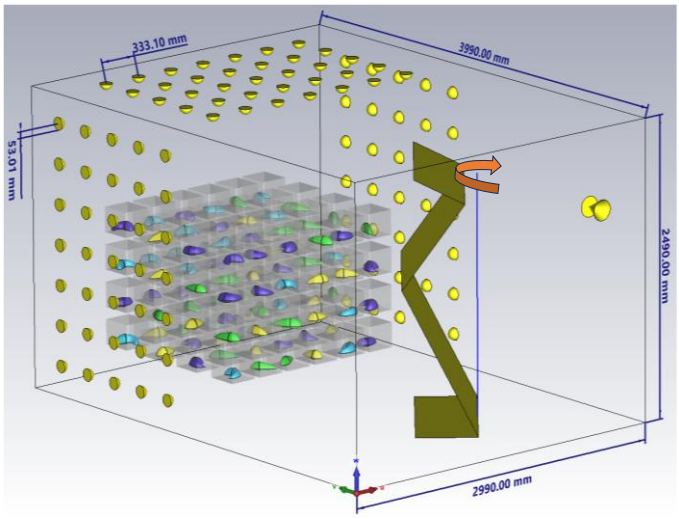

(a)

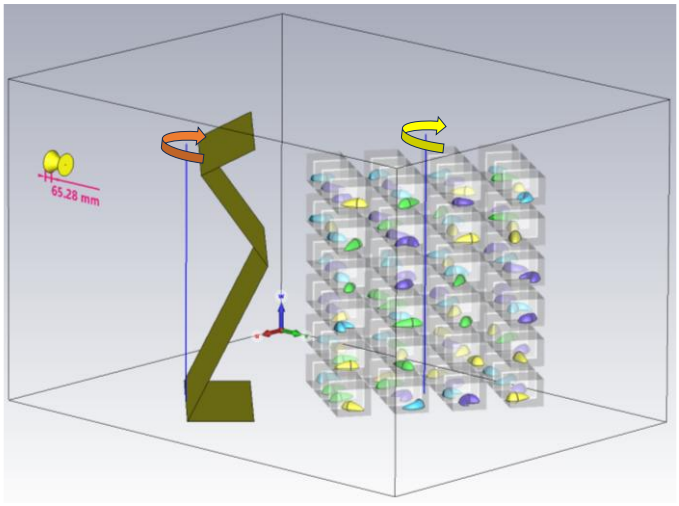

(b)

Fig. 1. UNIVPM-RC CST simulation models featuring (a) 6×4×4 (u, v, w) static (or translational dynamic) and (b) 4×4×6 rotational dynamic cage assemblies and discone antenna. The hemispherical field-diffusers depicted in (a) are grounded to the RC model ceiling and lateral walls.

C. Dosimetric Assessment

Following the MC framework outlined in [10], the rat model weights were randomly assigned according to a raised-cosine distribution, with an average mass of 650 g and a relative standard deviation (R-SD) of approximately 11%, which are representative of the NTP bioassay adult rats [3]. As done in [13], this study assigned a different random mass for each subsequent stochastic realization (i.e., mode-stirrer position) of the incident RC field. For each realization, each rat model posture was randomly chosen from the four predefined options (elongated, resting, sleeping clockwise or counter-clockwise); position and orientation within each individual cage were subsequently assigned.

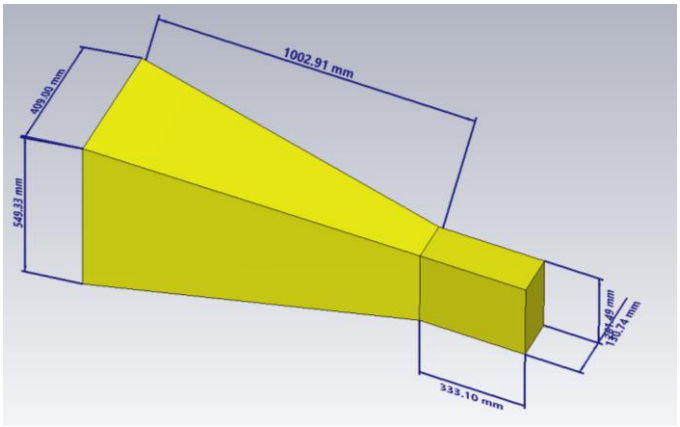

(a)

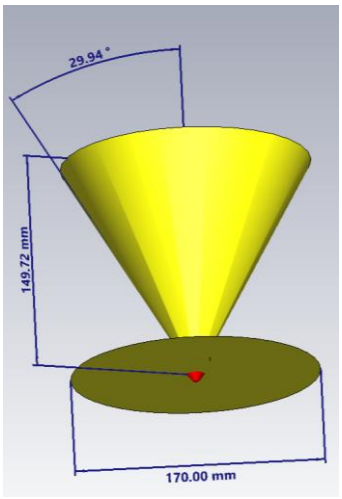

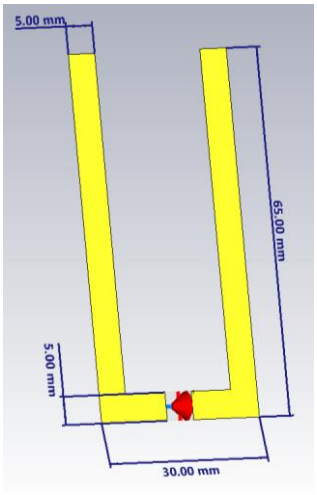

(b) (c)

Fig. 2. Simulation models of horn antenna (a), the discone (b) and the U-shaped dipole (c). Figure as from [13].

As mentioned, this study also addresses dynamic placement of the cage assembly, either translational or rotational, allowing in both cases the placement of 96 caged rat models. In the former case, the 6×4×4 cage assembly is randomly displaced by at most λ/2 in either direction along u and by at most λ/4 along *v*, with respective uniform probability density functions (PDFs), for each subsequent position of the RC mode-stirrer. Such a modest displacement range was motivated by practical considerations, anticipating the constraints likely imposed by the rats drinking-water system for example. In the latter case, the 4×4×6 cage assembly is rotated randomly around a vertical axis crossing its center, with uniform rotational angle PDF in [0,2π), for each position of the RC mode-stirrer. In both static and dynamic exposure cases, the individual and collective wbSAR statistics for the 96-rodent cohort were obtained from TLM and FEM simulations performed at 36 angles of the RC mode-stirrer, across a complete stirrer revolution. This methodology generated a comprehensive set of wbSAR values, enabling the calculation of cumulative probability distribution functions (CDFs) for both instantaneous and ensemble-averaged wbSARs (averaged across the range of stirrer angles).

In every studied RC configuration, we ran simulations stepping the RC mode-stirrer every 10 degrees, yielding 96×36 wbSAR values each, which were normalized by the net RF power into the antenna. Unlike in [10], where the rat model kept the same mass across stochastic realizations (only 96 mass values were in play), this study provided 3456 wbSAR-mass value-pairs for each RC configuration, thus yielding reliable estimates of the correlation coefficient between mass and wbSAR in real RCs.

III. Results

The Pearson correlation coefficient (PCC=-0.14) between instantaneous wbSAR and the corresponding rodent masses for the static RC configuration featuring the discone antenna (FEM solution) is reported in Fig. 3, showing 3456 wbSAR-mass value-pairs and the corresponding least-squares fitting line. This PCC value is markedly lower than those reported in studies that employed idealized Rayleigh fields synthesized via random PW superposition, e.g. PCC values around -0.71 were reported in [10]. Note that here wbSAR is normalized to the net RF power into the antenna in a realistic RC model, while it is normalized to the free-space squared incident electric field when using idealized Rayleigh fields.

Figure 4 depicts the histogram of the instantaneous wbSAR from the same RC configuration, which is well fitted with a lognormal-like PDF having the same mean and 38.8 % R-SD. This result is in general agreement with the findings in [10], [13]. The histogram for the cage-wise ensemble-averaged wbSAR is also reported in the figure (14.0 % R-SD).

Figure 5 provides a breakdown of the ensemble-averaged wbSARs versus cage distance from the RC stirrer and antenna for all the (non-rotational) 6×4×4 (*u,v,w*) RC configurations. With reference to Fig. 1(a), four different distances are determined when crossing each 6×1×4 subset of the whole cage assembly moving along the *v* axis. The reported values in dB scale indicate a consistent wbSAR decay farther from the antenna and stirrer, with an overall drop being about 1 dB. Such a uniform decrease across cages could not be observed when impressing idealized Rayleigh fields rather than simulating a realistic RC, since the random PW superposition would inherently enforce artificial symmetries.

As done in [10], a similar breakdown is shown in Fig. 6, for the same RC configurations, where subsets of cages were defined depending on whether they reside at the parallelepipedal cage assembly corners (8 cages), edges (32), faces (40), and inside locations (16). Also in this case, about 1 dB drop is observed among these subsets for the cage-wise ensemble-averaged wbSARs, indicating shading effects proportional to the number of cage faces obscured by other cages. Such an effect is more pronounced than the ~5% effect observed in [10] for the "day-long exposure" scenario, which is similar to this study insofar the rat models are allowed to switch posture and position at every random field realization.

The use of field diffusers and the spinning of the whole cage assembly were studied to determine whether they would mitigate substantially the aforementioned shortcomings.

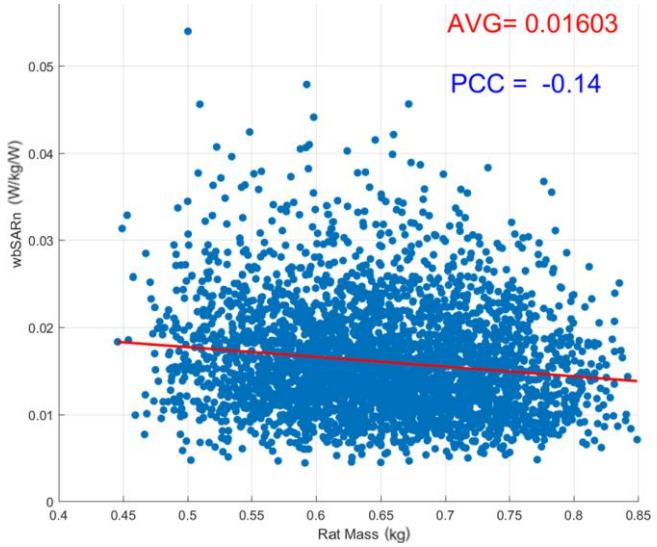

Fig. 3. Pearson correlation coefficient (PCC) between the instantaneous wbSAR and the corresponding rodent weights for one of the static RC configurations featuring the discone antenna (FEM solution). The wbSAR data set least-squares linear fit is depicted with a red line.

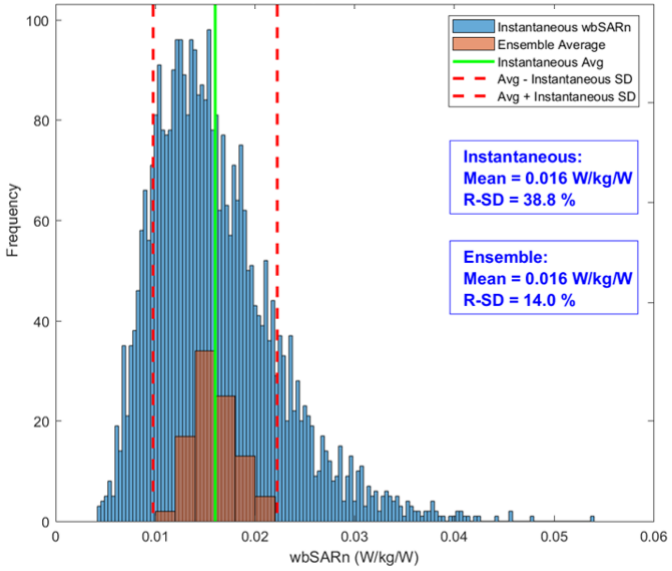

Fig. 4. Histogram of the instantaneous wbSAR, well approximated using a log-normal PDF (38.8 % R-SD), as well as of the cage-wise ensemble-averaged wbSARs (14.0 % R-SD), for the same RC configurations in Fig. 3.

However, while the effects of the aforementioned diffusers arrangement was modest, a quite positive impact was observed when random spinning of the 4 × 4 × 6 cage assembly about its vertical center axis was implemented in the MC analysis. In this case, the effects of distance from the stirrer and antennas are essentially eliminated for LoS (horn) as well as NLoS (discone) cases, as shown in Fig. 7.

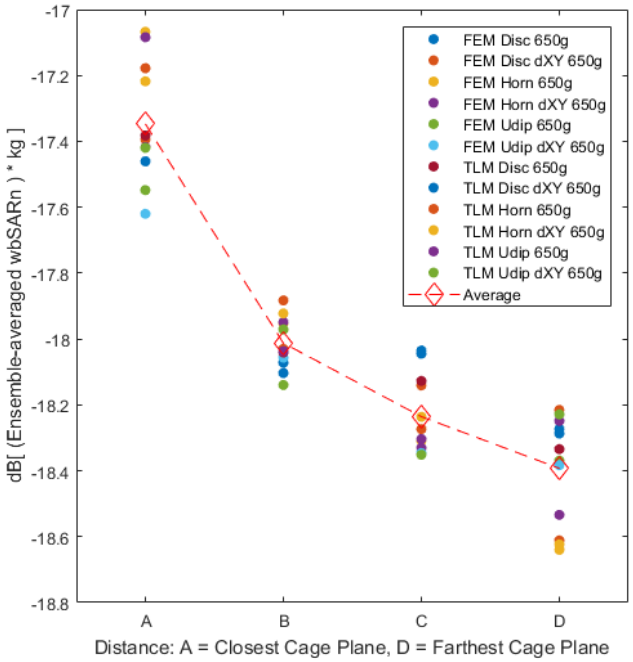

Fig. 5. Cage-wise ensemble-averaged wbSARs versus cage distance from RC stirrer and antenna for all the 6×4×4 (u,v,w) RC configurations, encompassing all three antennas, as well as FEM and TLM solutions. The label "dXY" indicates configurations involving random translations of the cage assembly.

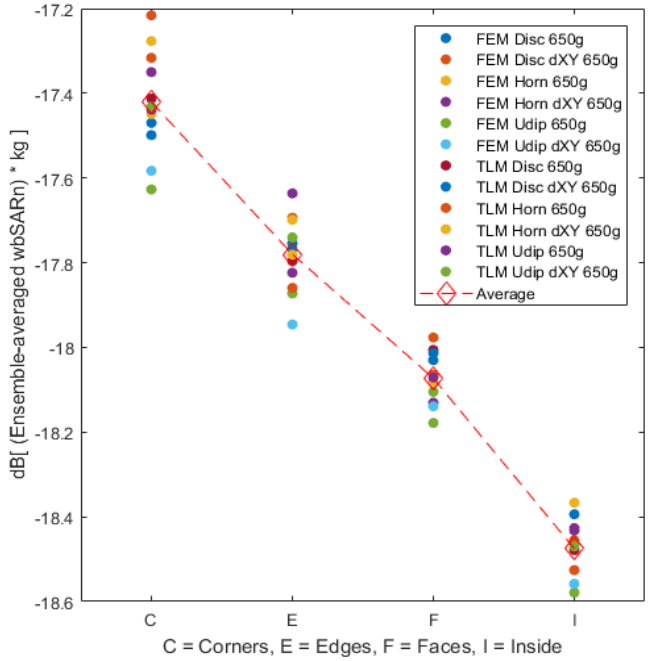

Fig. 6. Cage-wise ensemble-averaged wbSARs versus cage location: corners (8), edges (32), faces (40), and inside locations (16). The label "dXY" indicates configurations involving random translations of the cage assembly.

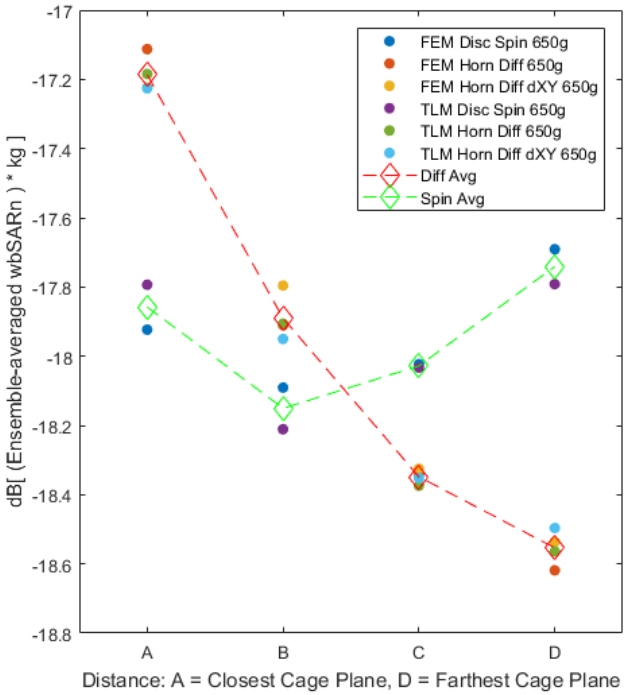

Fig. 7. Cage-wise ensemble-averaged wbSARs versus cage distance from RC stirrer and antenna for RC configurations, encompassing diffusers ("Diff") and spinning cage assembly ("Spin"), for both FEM and TLM solutions.

Table I summarizes the obtained results showing a significant narrowing of the cage-wise ensemble-averaged wbSAR distributions in spin cases (~ 10% R-SD) against those in no-spin cases (~ 15-18%).

Table 1. Summary of the cage-wise ensemble-averaged wbSAR distributions.

	Mean [mW/kg/W]	**Std Dev [mW/kg/W]**	**R-SD [%]**
FEM Diff	15.86	2.78	17.54
FEM dXY	15.86	2.46	15.51
FEM Spin	15.92	1.60	10.03
TLM Diff	15.97	2.86	17.90
TLM dXY	15.99	2.55	15.96
TLM Spin	16.01	1.55	9.66

IV. Conclusions

After demonstrating in [13] the feasibility of whole-RC computational dosimetry within a multivariate MC framework for large rodent cohorts at 900 MHz, in this study we focused on the thorough characterization of the uniformity of RF exposures, also expanding the use of diffusers and cage repositioning strategies within the UNIVPM-RC simulation model. The results indicated asymmetries in the cage-wise wbSARs, the extent of which had not been fully appreciated in prior studies employing idealized Rayleigh fields to model RCs. Furthermore, we documented a much lower correlation between wbSAR and rodent mass than previously observed in analogous studies employing idealized Rayleigh fields.

Attempts to improve the cage-wise ensemble-averaged RF exposure (in terms of wbSAR) allowed quantifying the impact of different approaches (horizontal translation or spinning of the cage assembly, as well as hemispherical diffusers on the RC walls), observing the most favorable effects for cage-assembly spinning.

References

[1] K. B. Jung, T. H. Kim, J. L. Kim, H. J. Doh, Y. C. Chung, J. H. Choi and J.-K. Pack, "Development and validation of reverberation-chamber type whole-body exposure system for mobile-phone frequency," *Electromagn. Biol. Med.*, vol. 27, no. 1, pp. 73-82, 2008.

[2] C. Li, L. Yang, B. Lu, Y. Xie and T. Wu, "A reverberation chamber for rodents' exposure to wideband radiofrequency electromagnetic fields with different small-scale fading distributions," *Electromagn. Biol. Med.*, vol. 35, no. 1, pp. 30-39, 2016.

[3] National Toxicology Program. "NTP technical report on the toxicology and carcinogenesis studies in Hsd: Sprague Dawley rats exposed to whole-body radio frequency radiation at a frequency (900 MHz) and modulations (GSM and CDMA) used by cell phones," Tech. Rep. no. NTP TR 595, 2018.

[4] National Toxicology Program. "NTP technical report on the toxicology and carcinogenesis studies in B6C3F1/N mice exposed to whole-body radio frequency radiation at a frequency (1900 MHz) and modulations (GSM and CDMA) used by cell phones," Tech. Rep. NTP TR 596, 2018.

[5] M. Capstick, S. Kuehn, V. Berdinas-Torres, Y. Gong, P. F. Wilson, J. M. Ladbury, et al., "A radio frequency radiation reverberation chamber exposure system for rodents," *IEEE Trans. Electromagn. Compat.*, vol. 59, no. 4, pp. 1041-1052, Mar. 2017.

[6] T. Wu, A. Hadjem, M.-F. Wong, A. Gati, O. Picon, and J. Wiart, "Whole-body new-born and young rats' exposure assessment in a reverberating chamber operating at 2.4 GHz," *Phys. Med. Biol.*, vol. 55, pp. 1619–1630, 2010.

[7] Y. Gong, M. H. Capstick, S. Kuehn, P. F. Wilson, J. M. Ladbury, G. Koepke, et al., "Life-time dosimetric assessment for mice and rats exposed in reverberation chambers for the two-year NTP cancer bioassay study on cell phone radiation," *IEEE Trans. Electromagn. Compat.*, vol. 59, no. 6, pp. 1798-1808, Dec. 2017.

[8] S. Jeon, W. Jang, A.-K. Lee, H.-D. Choi, J.-K. Pack, J. Wang, and D. Kim, "Distances between rats in reverberation chambers used for large-scale experiments," *J. Electromagn. Eng. Sci.*, vol. 21, pp. 148-52, 2021.

[9] R. Ito, S. Jeon, J. Wang, A.-K. Lee, J.-K. Pack, H.-D. Choi, Y. H. Ahn, and K. Imaida, "Quantification of exposure level in a reverberation chamber for a large-scale animal study," *IEEE J. Microw.*, vol. 2, no. 3, pp. 522-532, July 2022.

[10] V. De Santis, A. Di Francesco, K. R. Foster, G. Bit-Babik, and A. Faraone, "Monte-Carlo based numerical dosimetry in reverberation chamber exposure systems employed for In-Vivo rodent bioassays," *IEEE Access*, vol. 11, pp. 22018-22033, 2023.

[11] J. Chakarothai, J. Wang, O. Fujiwara, K. Wake and S. Watanabe, "Dosimetry of a reverberation chamber for whole-body exposure of small animals," *IEEE Trans. Microw. Theory Techn.*, vol. 61, no. 9, pp. 3435-3445, Sept. 2013.

[12] J. Chakarothai, J. Shi, J. Wang, O. Fujiwara, K. Wake, and S. Watanabe, "Numerical techniques for SAR assessment of small animals in reverberation chamber," *IEEE EMC Mag.*, vol. 4, pp. 57–66, Feb. 2015.

[13] A Faraone, G. Bit-Babik, P. Russo, A. De Leo, V. Mariani Primiani, and V. De Santis, "Computational RF Dosimetry of Rodents Cohorts in a Realistic Reverberation Chambers at 900 MHz," in *Proc. EMC Europe*, Bruges, Belgium, 2-5 September 2024.

[14] F. Moglie, A. P. Pastore, and V. M. Primiani, "Current probe characterization in a reverberation chamber," In *Proc. EMC Int. Symp.* 2005, Chicago, IL, USA, 2005, pp. 545-549.

[15] A. Di Francesco, V. De Santis, G. Bit-Babik, and A. Faraone, "An efficient plane-waves superposition method for improved spatial correlation accuracy in simulated reverberation chambers," *IEEE Access*, vol. 10, pp. 119641-119648, Nov. 2022.